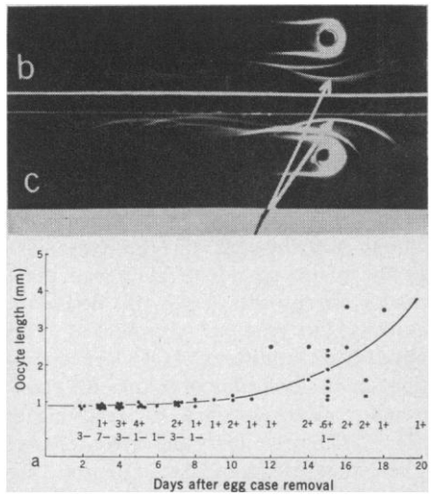

Fig. 3. (a) Initiation of egg maturation on removal of the egg cases in pregnant females (4 to 5 weeks) whose serums were subjected to electrophoresis. The number of animals which had the female specific protein in the hemolymph is indicated by a +. (b) Egg-maturing female. (c) Egg-maturing female 4 days after removal of the egg case. The arrows indicate the female specific protein.

cipitated in 10 percent trichloroacetic acid and then used for protein and radioassay. The specific activity of the total serum proteins of egg-maturing females was nearly three times that of allatectomized females (Table 1). The rate of the synthesis of the female specific protein in normal egg-maturing females was about as high as that of the other serum proteins together. The rate of synthesis of the nonspecific proteins was three times higher in the egg-maturing females than in allatectomized ones. Treatment of serums from allatectomized females with the antibody to female specific protein yielded no precipitate. Implantation of active corpora allata into allatectomized females with ligated necks caused both a high rate of synthesis of the female specific protein and an increase in the synthesis of the nonspecific protein (Table 1). Application of 1 μg of JH caused the *de novo* synthesis of the female specific protein at a somewhat higher rate than the implantation of four active corpora allata (*9*).

One can conclude that the corpus allatum hormone causes not only the *de novo* synthesis of a female specific protein but also increased general protein synthesis. Since the head was ligated in the allatectomized females, neurosecretion from the pars intercerebralis or hormones from the corpora cardiaca probably can be excluded as controlling agents of the observed protein synthesis. These results do not, however, negate any additional roles that those latter endocrine glands may play.

My data are in agreement with the hypothesis that the presence of the female specific protein is a prerequisite for egg maturation and not merely a concomitant of egg maturation. Additional observations strengthen this conclusion. The egg cases of females that had been pregnant for 4 to 5 weeks were removed, an interference that leads to a renewed egg maturation visible after about 8 to 12 days. Samples of serum were taken from these animals at daily intervals. Immunoelectrophoresis showed that some females had begun to produce the specific protein 3 to 4 days after removal of the egg cases (Fig. 3). This is 3 to 5 days before any traces of yolk deposition are detectable in the oocytes and before the accessory sex glands exhibit signs of activity. This finding corroborates analogous observations after treatment with JH; several days before yolk deposition begins, the female protein is present in the hemolymph. The importance of this protein for egg maturation is also suggested by the fact that more than 80 percent of the protein extractable from mature eggs is identical with the female specific protein (*6*). Although other nonspecific proteins contribute relatively little to the yolk, the fact that their synthesis is stimulated by the corpus allatum hormones suggests that they are essential in egg maturation.

FRANZ ENGELMANN
Department of Zoology, University of California, Los Angeles 90024

References and Notes

1. L. Hill, *J. Insect Physiol.* **8**, 609 (1962); K. C. Highnam, O. Lusis, L. Hill, *ibid.* **9**, 587 (1963).
2. W. Mordue, *ibid.* **11**, 617 (1965).
3. G. C. Coles, *Nature* **203**, 323 (1964); *J. Insect Physiol.* **11**, 1325 (1965).
4. F. Engelmann, *Arch. Anat. Microsc. Morphol. Exp.* **54**, 387 (1965); *Amer. Zool.* **5**, 673 (1965); F. Engelmann and D. Penney, *Gen. Comp. Endocrinol.* **7**, 314 (1966).
5. W. J. Bell, *Amer. Zool.* **8**, 755 (1968).
6. V. J. Brookes and R. K. Dejmal, *Science* **160**, 999 (1968).
7. The juvenile hormone is methyl-10-11-epoxy-7-ethyl-3, 11-dimethyl-10, 11-*cis*-trideca-2-*trans*-6-*trans*-dienoate.
8. I thank Dr. H. Röller, Texas A & M University, for supply of the juvenile hormone.
9. The amount of radioactivity precipitated by the specific and nonspecific antibodies does not always add up to the total radioactive precipitable by trichloroacetic acid, an indication that the hemolymph contains antigens for which no antibodies are available.
10. Supported by NSF grant GB-7365. I thank Dr. E. E. Sercarz for discussions concerning the immunological procedures, and Mr. F. Cartwright for technical assistance.

20 February 1969; revised 16 April 1969

Field Potentials Generated by Dendritic Spikes and Synaptic Potentials

Abstract. *Predictions from the cable model and equations for field potentials generated by single neurons are computed and compared with extracellular recordings from synaptically activated cerebellar Purkinje cell dendrites. Neither theory predicts the results, nor does the experimental situation satisfy the assumptions of either theory. Theoretical calculations from a recent formulation developed by Rall compare favorably with potentials recorded by other authors. Applications of these formulations are discussed.*

Some controversy has arisen over the interpretation of potentials recorded extracellularly from alligator cerebellar cortex (*1*). At issue is the applicability of the cable model of neurons as opposed to the volume conductor theory (*2, 3*). The problem is of interest as an example of the general difficulty of interpreting extracellularly recorded potentials from complex neural tissue. I will analyze the predictions of each theory and apply a new formulation developed by Rall and Shepherd (*4*) which overcomes many of the failures of the classical approximations.

Llinás *et al.* (*1*) have adduced evidence in favor of propagating dendritic action potentials. They stimulate electrically a surface sheet or beam of parallel fibers which form the main excitatory input to Purkinje cells and record extracellularly at various depths in the cortex. A negative wave appears and its latency is increased with deeper electrode placements. They contend that this progressive delay with increasing depth implies active propagation of spikes through the dendritic tree. A conditioning surface stimulus abolishes this transient response to a subsequent test stimulus, presumably via interneuronal inhibitory pathways. A slow surface-negative, depth-positive potential remains which is interpreted as an excitatory postsynaptic potential (EPSP). Inhibition may not only abolish spikes, but also can reduce the amplitude of some EPSP's and enhance others, depending on the postsynaptic geometry (*5*); hence this inhibitory effect cannot be used to determine whether the first wave is a spike or an EPSP. Other evidence contributes to the interpretation of the fast transient as a dendritic spike, but these supporting results are inconclusive, and Llinás

et al. feel that the field potential records are the major evidence for the existence of dendritic spikes.

Calvin and Hellerstein (*2*) argue that the cable model predicts the volume potentials in the present recording situation; Llinás *et al.* (*3*) use volume conduction analysis instead. Both groups appear to regard the slow bump remaining after inhibition of the fast negative transient as an EPSP. One would expect at least one of the above theories to predict the recorded field potential waveform and spatial behavior. This slow transient is replotted as Fig. 1A from a figure of Llinás *et al.* [figure 2B in (*1*)].

Calvin and Hellerstein (*2*) argue that the existence of a large isotropic volume of synchronously active cells of similar geometry eliminates the average transverse or laminar current. They therefore feel justified in applying the cable model to extracellular potentials as in the case of an isolated nerve, where intracellular and extracellular potentials are proportional (*6*), and they use this model to predict the field potentials in the vicinity of a system of neurons generating a passively conducted EPSP. They believe this prediction resembles Llinás' fast negative transient. They approximate the effect of brief EPSP's by the impulse response of the cable equation for an infinitely long cable (*7*):

$$V_m(X,T) = k_1 T^{-1/2} e^{-T - X^2/4T} \qquad (1)$$

where $V_m(X,T)$ is the membrane potential for an impulse at $T = 0$ and $X = 0$, $T = t/\tau$ is the time in membrane time constants, $X = x/\lambda$ is the axial or longitudinal distance in space constants, and k_1 is a constant. Rall (*8*) has shown that this formula applies even to a branching dendritic tree if certain reasonable geometries of branching are satisfied and λ is considered a function of x. In this report I take λ to be a constant; the graphical results could easily be adapted to a varying λ by locally scaling the x-axis. If Calvin and Hellerstein's assumption of intracelluar and extracellular proportionality holds, then this equation also represents the field potentials (*9*). This prediction is plotted as Fig. 1B in space and time.

The curves display only negative potentials at all depths, and a delayed, broader, and smaller peak with increasing depth. The slow transient data (Fig. 1A) fit only the last prediction. Even the fast negative transients, plotted as Fig. 3A [from figure 1C of Llinás *et al.* (*1*)], fail the crucial criterion of monopolarity (*10*). Furthermore, synchrony, symmetry, and zero average or local transverse current are not sufficient to justify application of the cable model to extracellular potentials. Consider two identical nerves placed parallel on filter paper soaked in Ringer solution separated by 2 cm and activated synchronously at one end; the net transverse current is zero, yet an electrode midway between the nerves records a volume conductor triphasic action potential, not the monophasic one predicted by the cable model. The cable model alone is inadequate for predicting the characteristics of the slow transient in the cortex.

Llinás *et al.* (*3*) apply volume conduction analysis, which predicts that a spike propagating through the dendrites of a single open-field neuron will appear as a triphasic transient at all depths below the surface, while an EPSP will reverse polarity as the electrode moves from current sink to source. They assume that the potentials from all the active Purkinje cells simply add. In the vicinity of an open-field neuron in a volume conductor, the field potential at a given point is very nearly proportional to the integral of membrane current divided by the distance to each membrane segment. Close to the nerve the local membrane currents predominate, so the potential will be nearly proportional to the current through the adjacent membrane (*11*). This current is proportional to the second spatial derivative of the membrane potential (*6*); therefore the EPSP field potential of a long dendrite expected under the assumption of Llinás *et al.* is proportional to the second spatial derivative of Eq. 1:

$$\frac{\partial^2 V_m(X,T)}{\partial X^2} = k_2 T^{-3/2}\left(\frac{S^2}{4T} - 1\right) e^{-T - X^2/4T} \qquad (2)$$

where k_2 is a constant determined by the geometry and tissue conductances (Fig. 1C).

The volume conductor predictions are biphasic in space, but some depth potentials are also strongly temporally biphasic, in contrast to the actual recordings (Fig. 1A). Also the spatial curves do not predict the mid-depth concavities seen in the slow transient. This formulation, then, also fails to account for some aspects of the data. The error in application can be understood if it is recalled that classical volume conductor theory applies only to the field induced by a single neuron in a charge-free medium. It is derived by solving Laplace's equation for the boundary condition of the nerve membrane surface potentials. Consider again the two synchronously active identical axons. Place a plane perpendicular to the neurons' plane, parallel to the neurons, and equidistant from them. The charge distributions on the two sides of the plane are identical; hence there can be no currents across this boundary and also no gradient of potential. This imposes an additional boundary condition on the solution of Laplace's equation for each neuron (*12*), resulting in altered field potentials and current flows. The currents from each neuron are now contained within the volume bounded by the imaginary plane. If the neurons are widely separated, this new boundary condition will perturb the original field only slightly, and volume conduction theory will still predict the results. If, however, there are not just two but many similarly oriented neurons packed tightly together and activated synchronously as in the cerebellar cortex, the extracellular current from each neuron is confined to the immediate region of the neuron. Now the actual as well as the average extracellular currents become almost purely axial, and one can approximate the extracellular medium as a series of resistors (*13*). These geometrical restrictions will cause the beam of activated Purkinje cells to act like a closed field where the field potential gradients in the beam are proportional to the Purkinje cell membrane gradients given by the cable model (*14*). Hence the unmodified single neuron volume conductor solution is not relevant to the present recording situation.

This analysis predicts a zero surface potential with respect to a distant electrode (*15*). The data contradict this prediction. However, if a secondary pathway is allowed to shunt current from the Purkinje cell somata through surrounding tissues to the distal Purkinje dendrites (see Fig. 2), the cerebellar surface will no longer be isopotential with infinity. The reference electrode sits somewhere on this secondary current pathway, which thus acts to divide the potentials generated according to cable theory in the activated beam. The secondary current pathway begins in the Purkinje cell layer, since deeper potentials are less positive, thus implying that current is flowing away from the sink (see Fig. 2). With Rall's procedure (*4*), the position of the reference lead on the divider

can be determined by the relative amplitudes of the positive and negative passively generated peaks in the recorded potentials and is here found to be four-sevenths of the electrical distance from distal dendrites to soma. To calculate the expected field potential at a point in the stimulated cerebellar cortex, the cable model is first used to predict the potential of the point relative to the locus of the impulse representing an EPSP, and then four-sevenths of the difference between the surface and soma level potentials is added to the cable potentials at each instant in time. This calculation requires an estimate of the effective length constant of the dendritic tree or the equivalent cylinder model introduced by Rall (*8*). I chose 300 μ as the value for λ that yielded the best fit of calculations to data. Since the dendritic tree is 300 μ long, this sets the cylinder length at 1 λ. Other values distort the potentials slightly and shift them along the x-axis. The field potentials predicted by this restricted current potential divider model are shown in Fig. 1D. The fewer zero crossings and nearly monophasic waveforms are also characteristic of the recorded potentials (Fig. 1A). The potential divider obscures the apparent propagation of the EPSP when potential is measured against time, and this explains the absence of any clear propagation of

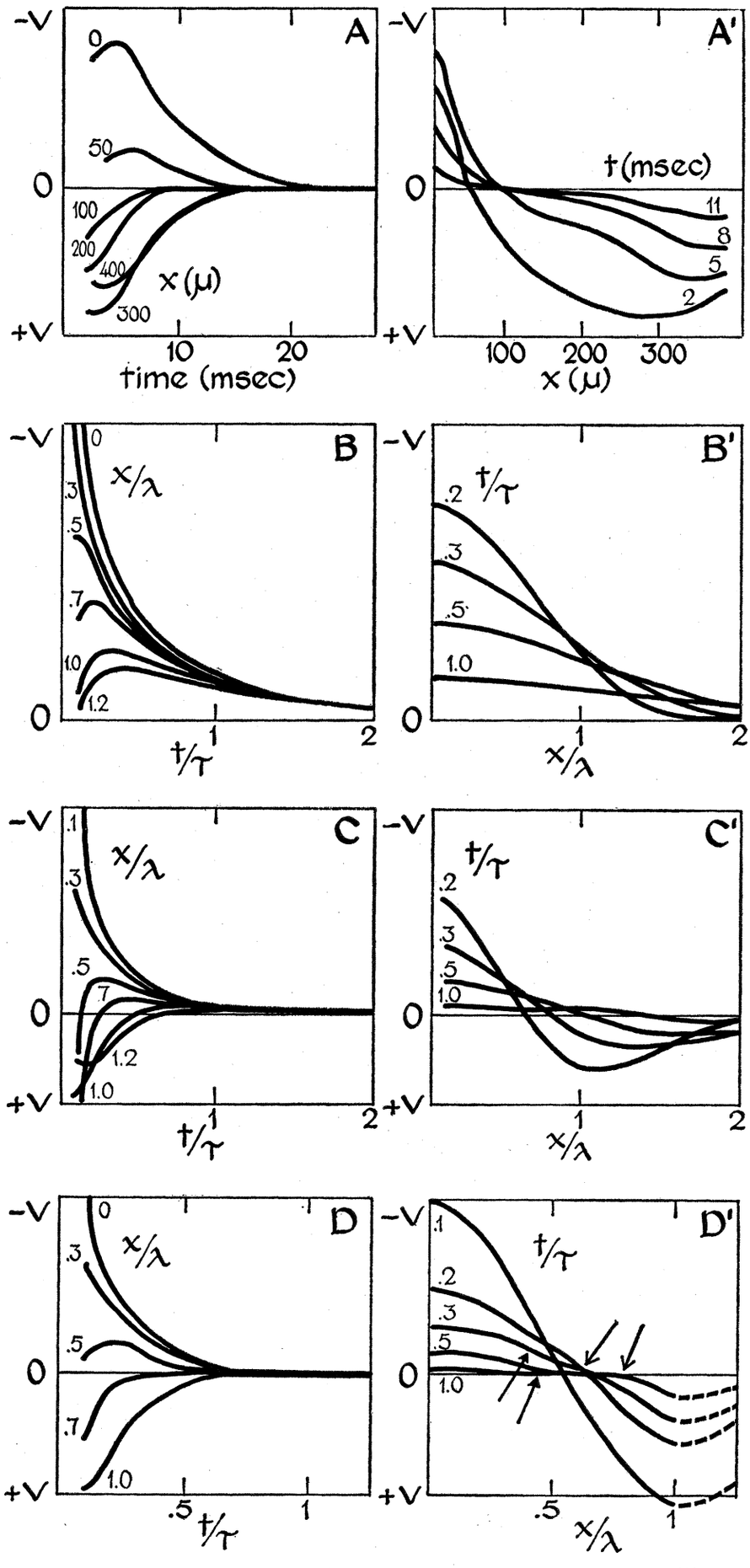

Fig. 1. (A) Field potentials recorded in the alligator cerebellar cortex following electrical stimulation of the surface parallel fiber input to the Purkinje cells [from (*1*)]. These potentials represent the slow transient following stimulation when the fast transient has been blocked by a conditioning stimulus. (B) Field potentials predicted by the impulse response of the cable model where the reference electrode is assumed at a great axial distance from the recorded activity. (C) Field potentials predicted by the impulse response of a cable placed in an infinite charge-free medium where the reference electrode is at infinity. (D) Field potentials predicted by the impulse response of a restricted current potential divider model, with the reference electrode at four-sevenths of the electrical distance from the distal dendrites to the somata of the Purkinje cells along the secondary extracellular current pathway (see Fig. 2). The dotted lines here and in Fig. 3 refer to recordings below the region of the dendrites, along the secondary current pathway. In (B) through (D), no effort is made to predict the absolute amplitudes of the voltage, since this calculation involves knowledge of the intra- and extracellular conductances. In all drawings, potential is plotted versus time at different depths on the left, and versus depth at different times on the right.

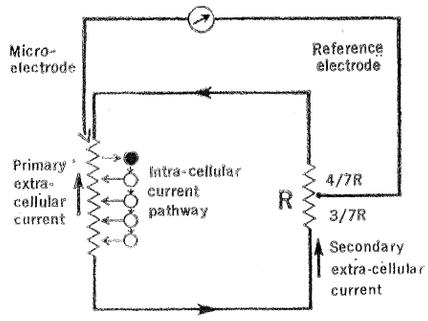

Fig. 2. Diagram showing the pathways for the current generated by a single dendritic tree activated synaptically at the distal tips. Current flows into the darkened compartment where there is an active excitatory synapse, and outward from the passively depolarized proximal compartments. See text for further explanation.

the EPSP slow transient. Evidently this recording situation makes interpretation of potential latencies extremely tenuous, especially for passive events. Moreover, the potential divider introduces mid-depth upward and downward concavities (filled and open arrows in Fig. 1D) in the spatially plotted field potentials which account for this otherwise anomalous property of the recorded potentials (*16*).

If this application of Rall and Shepherd's restricted current potential divider formulation is appropriate to the particular geometry, circuitry, and stimulation of the present case, the theory should predict the field potentials in a system of electrically excitable dendritic trees as well. In order to make such calculations, the dendrites are modeled as compartments whose conductances display kinetic properties similar to those of the Hodgkin-Huxley equations (*17*). The calculations require that the compartments be coupled by a safety factor, that the number of compartments and the space constant of the chain be known, and that a stimulus be specified (*4*, *18*). Such calculations would be very tedious. However, in their analysis of olfactory bulb field potentials (*4*), Rall and Shepherd give the predicted field potentials in antidromically invaded synchronously active parallel dendrites of chain length of 1λ, where the dendrites are electrically excitable. The curves from his figures [figures 8C and 10C in (*4*)] are replotted as Fig. 3B. These curves are for a system of neurons in spherical symmetry, with a potential divider reference of one-fourth, where an action potential enters the dendrites from the soma. The case of antidromically invaded olfactory bulb dendrites is somewhat different from the orthodromically invaded linear array treated here. Nevertheless, the similarity of these predictions to the fast negative transient in Llinás' recordings (Fig. 3A) is striking. In both calculated and experimental families of curves, one sees not only the delayed latencies and broadened smaller peaks that Calvin and Hellerstein attribute to EPSP's, but also the triphasic waveforms, propagated spatial maximums, and zero crossings in time and space that only actively propagated spikes would display. This analysis, then, does distinguish spikes from EPSP's, and identifies the fast transient rather unequivocably as an active spike, as concluded originally by Llinás *et al.* (*1*).

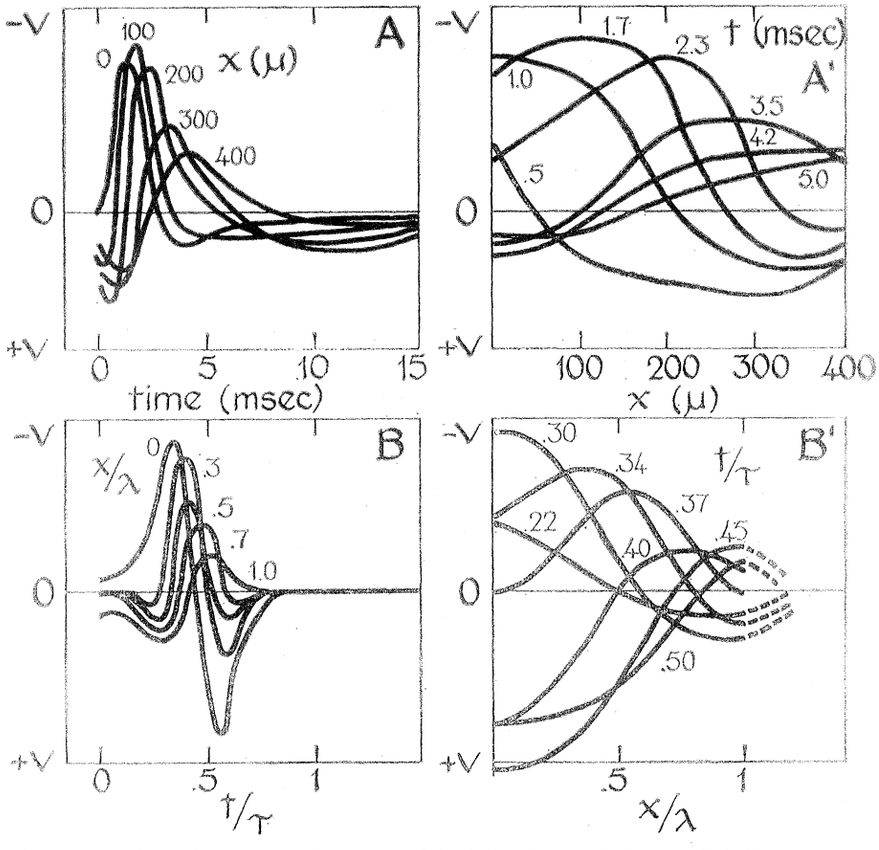

Fig. 3. (A) Cerebellar cortex field potentials following a single parallel fiber stimulus [from (*1*)]. These are the fast transients or dendritic spike potentials. (B) Field potentials predicted by the restricted current potential divider model where a spike is propagating antidromically out excitable dendrites. These curves are replotted from Rall and Shepherd (*4*) and are from a model with geometrical and potential divider parameters somewhat different from those most appropriate to the experimental situation. I invert Rall's *V*- and *x*-axes to account for an opposite propagation direction and polarity convention.

I do not wish to insist on the complete generality of this new formulation. For example, the deflections in Llinás' data representing the parallel fiber presynaptic spike volley are accurately and validly represented by classical volume conduction models. This is because these potentials result from a suddenly activated nerve sheet of small extent where the active electrode is at a point in a passive resistive medium accessible to the membrane current of each axonal compartment and the reference lead is in the same medium at a great distance. Similar considerations apply to recordings made lateral to the activated beam reported in a more recent paper by Llinás *et al.* (*19*).

It is clear, however, that neither the cable model for membrane potential nor the Laplace equation solution for one neuron in a volume conductor can always be applied without modification to fields surrounding neurons with complex geometries and coordinated activity. The activity of each neuron places boundary conditions on the action currents of other neurons, and, unless these conditions can be specified, analysis is difficult indeed. The present example stresses the need for carefully examining the assumptions in-

herent in any mathematical model before applying the model, and indicates that the recent formulation by Rall may be useful in the analysis of synchronous activation of units that have linearly ordered structural symmetry about the recording electrode.

ROBERT S. ZUCKER
Department of Biological Sciences and Neurosciences Program, Stanford University, Stanford, California 94305

References and Notes

1. R. Llinás, C. Nicholson, J. A. Freeman, D. E. Hillman, *Science* **160**, 1132 (1968).
2. W. H. Calvin and D. Hellerstein, *ibid.* **163**, 96 (1969).
3. R. Llinás, C. Nicholson, J. A. Freeman, D. H. Hillman, *ibid.*, p. 97.
4. W. Rall and G. M. Shepherd, *J. Neurophysiol.* **31**, 884 (1968).
5. J. C. Eccles, *The Physiology of Synapses* (Academic Press, New York, 1964), p. 172.
6. R. Lorente de Nó, *Stud. Rockefeller Inst. Med. Res.* **131**, 442 (194
A. L. Hodgkin and W. A. H. Rushton, *Proc. Roy. Soc. London Ser. B* **133**, 444 (1946); R. E. Taylor, in *Physiological Techniques in Biological Research*, W L. Nastuk, Ed. (Academic Press, New York, 1963), vol. 6, pp. 219–262.
7. This corrects an error in the function published by Calvin and Hellerstein. The equation is derived as the time derivative of the step response of the cable equation [see (*6*)].
8. W. Rall, *Ann. N.Y. Acad. Sci.* **96**, 1971 (1962); *Biophys. J.* **2** (No. 2, part 2), 145 (1962).
9. The k_1 now depends on the intracellular and extracellular resistivities and the dendritic tree cross-sectional area relative to the total area.
10. In addition, the cable model EPSP curves show a delay in latency to peak with increasing depth, but no shift in location of spatial peak. Even if one could accept this analysis on other grounds, it does not account for the shift in spatial position of the peak observed in the fast transient or presumed spike recordings of Llinás *et al.* Hence the theory developed by Calvin and Hellerstein does not agree with the data it was meant to explain.
11. R. Lorente de Nó, *Stud. Rockefeller Inst. Med. Res.* **132**, 384 (1947); C. F. Stevens, *Neurophysiology: A Primer* (Wiley, New York, 1966), pp. 161–173. Stevens shows that the field potential expression includes a term for the surface potential as well as the membrane current. Figures 1 and 5 of Clark and Plonsey (*13*) permit comparison of the membrane current and field potential distributions; they are quite similar, so it seems permissible to neglect the potential term and substitute the local membrane current for the weighted integral of all membrane current.
12. J. D. Jackson, *Classical Electrodynamics* (Wiley, New York, 1965), p. 16.
13. This analysis was first provided by Rall and Shepherd (*4*). The effect of boundary conditions on extracellular potentials was studied by J. Clark and R. Plonsey [*Biophys. J.* **8**, 842 (1968)]; they showed that a current-restricting boundary will confine action currents to longitudinal pathways and triphasic spikes become almost monophasic.
14. Contrast this result to that of Calvin and Hellerstein: By assuming proportionality between membrane and field potentials, not gradients, they arbitrarily set the zero point of the field potentials at infinity and assign this as the location of the reference electrode.
15. R. Lorente de Nó, *J. Cell Comp. Physiol.* **29**, 207 (1947).
16. All three models fit the data best if a time constant of 15 to 20 msec is used. This is in part due to the use of an impulse to represent an EPSP; the exact EPSP responses of all models would be slower and would fit the recordings with a time constant of about 10 msec. Note that the restricted current potential divider model predicts a space constant of 300 μ; the others fit for $\lambda =$ about 150 μ.
17. A. L. Hodgkin and A. F. Huxley, *J. Physiol.* **117**, 500 (1952).
18. W. Rall, in *Neural Theory and Modeling*, R. F. Reiss, Ed. (Stanford Univ. Press, Stanford, 1964), pp. 73–98.
19. R. Llinás, C. Nicholson, W. Precht, *Science* **163**, 184 (1969).
20. I thank D. Hartline, D. Kennedy, D. Smith, P. Stein, and D. Wilson for valuable discussions. Supported by the National Science Foundation.

28 February 1969; revised 14 April 1969 ■

Temporal Order Judgment and Reaction Time

Abstract. *A model which predicts judgment of the temporal order of stimuli from simple reaction time is proposed. Visual data show covariation of the two measures with luminance changes, and suggest that (i) temporal order judgments reflect a biased response criterion and (ii) the motor component of reaction time has little variability relative to variance in receptor system latency.*

One measure of the relative latency of two receptor systems is obtained from judgments by subjects of the temporal order of occurrence (TO) of stimuli separated by a small time interval. Interstimulus intervals that yield maximum uncertainty about which stimulus was presented first are held to reflect typical receptor system latency differences (*1*). Simple reaction time (RT) is also a measure of receptor system latency and should yield comparable inferences about latency differences between stimuli. A previous study (*2*) compared RT and TO data from heteromodal stimuli and found a considerable discrepancy between typical latency differences inferred from the two measures. Our report demonstrates a direct covariation between RT and TO with ipsimodal stimuli, and proposes a common underlying theoretical framework which allows a prediction of the TO performance from simple RT to the same stimuli.

The essential features of the theoretical proposal are shown in Fig. 1. Densities corresponding to receptor system latencies to the two stimuli are presented one above the other, with the convention that the origin of the time scale is located at presentation of stimulus 1. In this example the interstimulus interval, τ, is negative, meaning that stimulus 2 is presented first, and so the latency density, f_2 (t_2), for

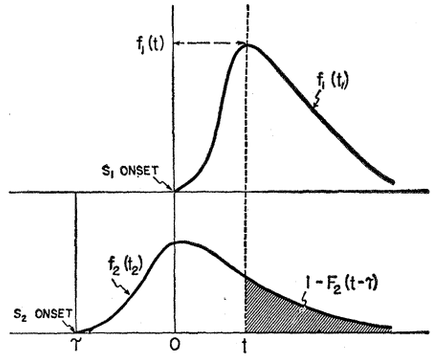

Fig. 1. Densities for detection latencies after stimulation from two sources, offset by the interstimulus interval, τ. Hatched area is the probability that the latency for stimulus 2 exceeds a latency of t for stimulus 1.

stimulus 2 has been shifted τ units to the left. Three assumptions are sufficient to produce a prediction of the psychometric function relating the probability of a stimulus 1 report to τ. (i) Receptor system latencies are independent of each other; (ii) neither distribution is changed by changes in τ; and (iii) the subject reports "stimulus 1 first" whenever on a particular trial stimulus 1 latency is exceeded by stimulus 2 latency plus τ. That is, the subject reports physiological asynchrony as physical asynchrony and has no difficulty in discriminating which input system was first.

Under these assumptions for an arbitrary input latency, t, from receptor system 1 (dotted line in Fig. 1), the probability of a stimulus 1 report is simply $1 - F_2(t - \tau)$. This formulation is appropriate for positive values of τ as well, as the latency distribution functions are zero for negative arguments. Weighting each probability by the density of t, and integrating, we find

$$P_\tau(\text{"S1 first"}) \equiv F(\tau) = \int_0^\infty f_1(t)\,[1 - F_2(t - \tau)]\,dt \quad (1)$$

where $F(\tau)$ is the cumulative form of the latency difference distribution (*3*). The decision rule might have been stated as the following: the subject reports "stimulus 1 first" whenever $t_1 - t_2 < \tau$. Varying τ produces different criterion values and the decision procedure is the same as that described for the two-alternative forced-choice situation in signal detection theory (*4*). The mean and variance of the difference distribution are the difference